Supernova Remnants: acceleration of particles and gamma-ray emission

H.J. Völk
Max-Planck-Institut für Kernphysik, Postfach 10 39 80, D-69029 Heidelberg, Germany

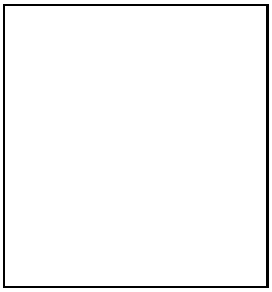

Particle acceleration in the dynamically evolving environment of Supernova Remnants is discussed in the framework of a genuinely time-dependent nonlinear theory, assuming spherical symmetry. As a consequence the dependence of injection on the angle between shock normal and external magnetic field direction requires a renormalisation of the calculated particle fluxes. The recent observational results in TeV gamma-rays from such objects are discussed and found to be consistent with theory. We conclude that for the present instrumental sensitivities there are no reasons to draw premature negative conclusions as to the possible origin of the Galactic Cosmic Rays below the "knee" in Supernova Remnants. In addition, theoretical predictions and observations are getting very close. Therefore the coming generation of ground-based and space-borne detectors will decide this basic question of astrophysics.

1 Introduction

Supernova (SN) explosions in the ensemble of stars constitute the largest, "steady" mechanical energy input in galaxies. They release an amount $E_{SN} \approx 10^{51}$ ergs of mechanical energy per event, at a rate of 1 event per 30 to 100 yrs in the Milky Way. Supernova Remnants (SNR) are also the largest heat source for the Interstellar Gas, and have long been speculated to be the dominant accelerators of the so-called Galactic Cosmic Rays (CRs). It is the latter question which we shall discuss here.

We begin with a review of particle acceleration in the outer SNR shock wave that communicates the explosion energy to the ambient medium. We shall in particular discuss the injection process, and will argue that spherically symmetric models are incomplete without a renormalisation of the calculated particle fluxes. High energy γ-ray emission due to inelastic collisions of the energetic particles with gas nuclei or background photons is an observational consequence of particle acceleration. We shall therefore critically evaluate the recently available observational results in TeV γ-ray emission from the young objects SN 1006, SNR RX J 1713-3946, Cas A, and Tycho's SNR. Several older objects, like IC443 or γ-Cygni, are observationally still too complex to draw general conclusions.

Finally, we shall turn to the observations of the diffuse γ-ray emission from the Galactic disk. At TeV energies it might be interpreted as the unresolved sum of individual γ-ray sources in the form of CR sources. These may be SNRs or other objects, and we may be able to identify them in other wavelength ranges, like the radio continuum. Thus, apart from a rather well-known truly diffuse background contribution,

the spatial distribution of this "diffuse" TeV γ-ray emission should be compared with the known SNR distribution in the Galaxy and, mutatis mutandis, its energy spectrum ought to correspond to the inferred *average* CR source spectrum.

2 Particle acceleration in SNRs

The γ-rays from SNRs stem from particles that have at some time in the past been accelerated at the outer SNR shock to a momentum distribution that is nonthermal; it corresponds to a power law $\propto p^{-\beta}$. In fact, the number density n_i of particles participating in the acceleration process, the injection fraction, is quite small compared to the thermal particle density n_{th}, with $\eta = n_i/n_{th} \approx 10^{-4}$. In one plausible picture [2,3,5,6] - see however[8] for a different view - the injected ions are those which are able to escape from the shocked (i.e. suddenly decelerated and heated) downstream thermal distribution along the magnetic field into the incoming plasma region upstream of the shock, where they excite MHD waves ("Alfvén waves") and thus initiate the diffusive acceleration process.

These scattering waves[9] keep the particle distribution close to isotropic, and in the process particles are stochastically scattered back and forth across the shock front many times, gaining energy in each shock crossing, before being convected downstream together with the scattering wave field. This picture holds in its simplest form for nonrelativistic shocks, i.e. for the case in which the difference in flow speed across the shock front is nonrelativistic. In any conventional view SNR remnants fulfill this condition, and in the sequel we shall confine our attention to this case.

Apart from the fundamental aspect of the excitation of scattering waves by the accelerating particle component itself, shock acceleration can also be described in terms of a well-known transport equation for the isotropic part of the distribution function that contains the mechanisms of adiabatic energisation/deceleration, spatial diffusion and convection. This diffusive shock acceleration process has been reviewed extensively in the past, e.g. [10,11,12].

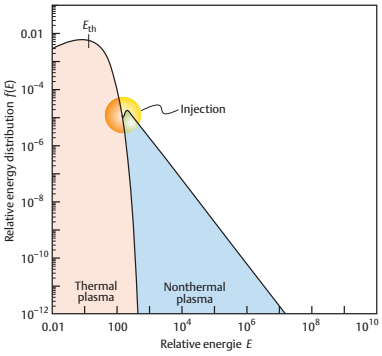

Figure 1: Particle energy distribution at the shock (arbitrary units). The downstream thermal plasma has a quasi-Maxwellian distribution with thermal energy E_{th}, whereas above a somewhat larger energy (injection) the accelerated nonthermal distribution starts to dominate.

In order to go beyond the test particle limit, it is apparently necessary to include the energy and momentum exchange of the scattering particles with the thermal gas (plasma) and the wave field in the calculation of the *overall* dynamical evolution of the system. Then, for a strong shock, the downstream nonthermal and thermal energy densities turn out to be comparable, $E_{nonthermal} \sim E_{thermal}$. This means that the process can be highly nonlinear and efficient[4]; for a very recent review, see [7]. The differential energy distribution in the relativistic range is close to a E^{-2} -law, i.e. it contains essentially equal energy per decade in particle energy E. The ratio of the energy densities and the spectrum are both rather close to what is observed for the CRs in our Galaxy and in many astronomical objects which exhibit nonthermal emission.

All this pertains to nuclei which are known to dominate electrons in the Galactic CRs by a factor of ~ 100. However, the large Thompson cross section allows the electrons to radiate very effectively, and therefore they play a significant role for the nonthermal emission from SNRs [13] and other nonthermal sources.

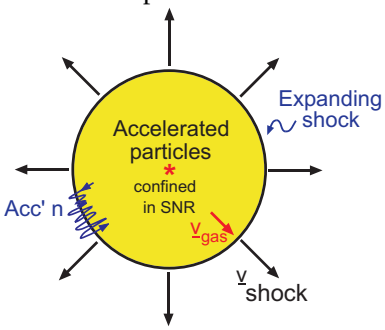

Figure 2: At the spherical SNR particles are injected from the inside and remain diffusively confined after acceleration, expanding with the thermal gas until its velocity v_{gas} decreases below characteristic ambient velocities.

The special characteristics of SNRs lie in the fact that they are the result of a strong point explosion. Therefore they are intrinsically time dependent objects, to lowest order spherically symmetric, and indeed strongly nonlinear accelerators. Particles that have been accelerated remain inside the expanding remnant, undergoing adiabatic expansion losses and diffusive transport in the interior, before being ultimately released into the Interstellar Medium when the remnant gets old and starts to decay (Fig. 2).

2.1 Volume-integrated particle, γ-ray spectra, and energies

In the simplest case of a uniform Interstellar Medium, the external magnetic field B is uniform and thus the angle Θ_{nB} between the shock normal and B varies systematically over the shock surface. Assuming for simplicity nevertheless spherical symmetry for the solution of the nonlinear acceleration problem, not only the acceleration process is calculated for a "parallel shock" ($\Theta_{nB} = 0$), but also the injection efficiency is assumed to be the same over the entire shock surface, indeed equal to that for $\Theta_{nB} = 0$. Whereas the first approximation is possible for almost all values $\Theta_{nB} \neq 0$, e.g. [10], this is not true for the injection rate, e.g. [1, 3], and we shall argue that this requires a renormalisation of the spherically symmetric result. For the case of a uniform ambient medium, typically appropriate for SNe type Ia and core collapse SNe type II from precursor stars considerably less massive than $20M_{\odot}$, the nonlinear set of equations describing nucleon acceleration and the dynamical backreaction on the thermal gas has been solved numerically [14, 15], covering the complete time evolution. Fig. 3 shows an example of the momentum distribution of energetic protons, spatially integrated over the SNR volume [15].

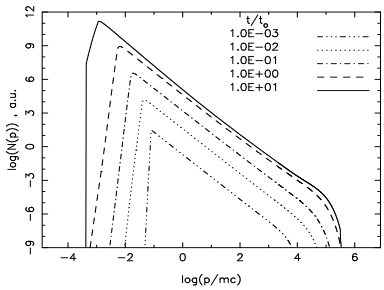

Figure 3: (a) Volume-integrated proton momentum spectra $N(p)$ for different SNR ages t in units of the sweep-up time $t_0 = 1893$ yr, for an injection fraction $\eta = 10^{-4}$, upstream density $n = 0.3$ H-atoms cm^{-3}, $E_{SN} = 10^{51}$ erg, ejected mass $M_{ej} = 10M_{\odot}$, and $B = 5\mu$G.

Above the injection momentum the integrated spectrum is close to a power law which is getting harder towards the cutoff due to nonlinear shock modification; the overall average spectral index is close to 2; the maximum momentum reaches about

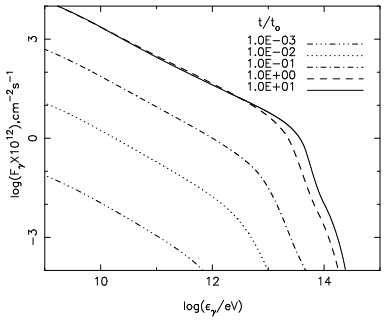

Figure 4: Volume-integrated π^0-decay γ-ray spectrum corresponding to the parameters of Fig. 2.

$3 \times 10^{14}\mathrm{eV}/c$ at late times for the particular parameters chosen [15]. (As a side remark: radio synchrotron electrons, with typical energies as low as 10 GeV, should therefore have a somewhat steeper spectrum for the nonlinearly modified, very strong shocks characterising young remnants [18, 19]; in fact, the observed radio spectral index often exceeds the value 0.5 that would correspond to the spectra at high momenta)

Of similar interest is the volume-integrated integral γ-ray spectrum from the SNR due to π^0-decay from inelastic collisions with thermal gas nuclei, Fig. 4. For a spatially resolved observation one has, of course, to compare the locally calculated emission.

Another aspect of the time-dependent evolution can be recognised in the different components of the volume-integrated energy in the system, Fig. 5. Whereas initially the entire hydrodynamic energy is in the ejected mass, the thermal and kinetic energies of the gas and the energy E_c in accelerated particles increase as a function of time. E_c is greater or about equal to the other energy components in the Sedov phase, reaching a value $E_c/E_{SN} \approx 0.5$ in the late Sedov phase, when particles should be released [15].

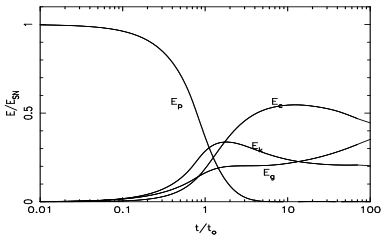

Figure 5: Volume-integrated energy fractions for the parameters of Fig. 3. The quantities E_p, E_g, E_c, and E_k correspond to ejecta energy, gas thermal energy, CR energy, and gas kinetic energy, respectively.

CR observations on the other hand suggest a significantly lower *average* source efficiency. Indeed, according to standard estimates [51], the energy input into CRs from an individual SNR is about $(dE/dt)_{Sources} \approx 0.1 \times \nu_{SN} E_{SN}$, and we shall use this number in the sequel.

2.2 Renormalisation of integral γ-ray fluxes

The physical reason for the overproduction of nonthermal energy in the spherically symmetric model lies in its assumption of a constant injection efficiency over the shock surface. This is actually not the case. To lowest order the mean magnetic field configuration for a point-like energy input into an environment with a uniform field looks like the cartoon in Fig. 6: The external magnetic field lines are refracted into the interior. The minimum field-aligned speed of a downstream particle required to outrun the radially propagating shock wave into the upstream plasma along a field line is proportional to $\cos^{-1}\Theta_{nB,2}$ and appears in the (quasi-exponential) tail of the velocity distribution of the shocked downstream plasma.

In reality, the magnetic field in the collisionless (sub)shock is much more complicated, even in the "parallel" case $\Theta_{nB,1} = 0$[2,5]. As a rough approximation we may nevertheless scale the injection velocity with the factor $\cos^{-1}\Theta_{nB,2}$ which dramatically reduces the injection rate for increasing shock obliquity.

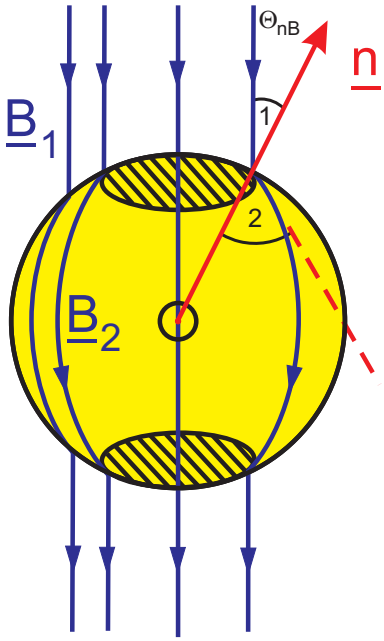

Figure 6: Cartoon of the B-field refraction in a SNR situated in a uniform field region. The angle $\Theta_{nB,2}$ between the downstream field $\underline{B_2}$ and the shock normal direction $\underline{n}$ becomes so large beyond the hatched "polar" region that injection is effectively inhibited.

We shall not go into the details here. However, it is clear that for a sizeable fraction of the shock surface near the "equator", $\cos\Theta_{nB,1} = 0$, particle acceleration will be inefficient relative to that in the regions near the "poles".

To lowest order, the spatial integral of the accelerated spectrum should therefore be reduced by multiplying the spherically symmetric result with a *renomalizing factor* given by the ratio of shock surface area with efficient injection to the total shock area. Instead of such a theoretical factor we shall use here an even simpler prescription. This is an *empirical* renormalization factor, on the assumption that SNRs are indeed the sources of the Galactic CRs, and corresponds to the ratio of the expected value $E_{c,\,observed}/E_{SN} \approx 0.1$ to the calculated value of E_c/E_{SN}. For the case of Fig. 5 it is about 1/5.

3 Observed young SNRs

3.1 SN 1006 in the Southern Hemisphere

Being a bright radio synchrotron source, this historical remnant of a SN type Ia has also been detected in nonthermal X-rays[16,17], believed to be synchrotron emission. The X-ray morphology is characterized by two symmetrically situated emission regions of unequal strength, reminiscent of the "polar" regions of preferred injection discussed before. Given the implied high electron energies of ~ 100 TeV[20] and assuming magnetic fields below $10\ \mu$G , SN 1006 was consequently also predicted as an Inverse Compton (IC) γ-ray source by[21,22,23]. A TeV γ-ray detection was finally reported by the Japanese/Australian CANGAROO collaboration[31]. The report contained also indications of a γ-ray morphology resembling that in nonthermal X-rays.

Using the popular estimate[24,25] of the expected π^0-decay emission for the parameters of SN 1006, it turns out[26] that the CANGAROO flux is more than a factor of about four higher than this estimate, making a hadronic γ-ray source implausible for the given parameters. A detailed recent kinetic modeling of the nonthermal X-ray and γ-ray emission[27] raises the π^0-decay luminosity by a factor ~ 2, making it comparable to the IC γ-ray luminosity. However, as argued above, this flux should be renormalized - by a factor of ~ 6 - which once again appears to rule out a hadronic origin. [28] have presented a more phenomenological discussion which in particular points out that the implied γ-ray morphology fits much better a shell-type hadronic γ-

ray emission rather than an IC emission that they expected to be rather uniform across the remnant, given the uniformity of the target photon distribution. On the arguments from Fig. 6 however, a nonuniformity of the γ-ray emission is expected in any case since the particle distribution is asymetric.

Given the present experimental results, much depends on the strength of the effective magnetic field in the acceleration region. There is clearly a need to observe at lower and higher γ-ray energies than 1 TeV with more sensitive instruments to obtain precise spectral information, especially about γ-ray cutoffs, in order to allow a distinction between a nucleonic and an IC origin of the γ radiation. At the same time, the available improvements in spatial resolution will be important in order to obtain a clear γ-ray morphology for this large remnant of $\approx 0.5^\circ$ diameter.

3.2 SNR RX J1713.7-3946 in the Southern Hemisphere

This large, 1° diameter SNR had been discovered in the *ROSAT* All-Sky Survey[33] and was observed as a strong nonthermal X-ray and radio source[29,30]. In fact, SNR RX J1713.7-3946 is the only SNR that does not show significant evidence for thermal X-ray emission from any portion of the remnant! It has been reported as a TeV γ-ray source by CANGAROO[32]. However, the parameters, like distance, circumstellar environment, and age, are not well known. In particular, the distance has been estimated as widely different as 1 kpc [29] and 6 kpc [30], at gas densities of 0.28 H-atoms cm^{-3}. The latter authors also concluded that the progenitor should have been a massive star, in whose wind-blown bubble the SNR shock still propagates today.

If the reported γ-ray emission is interpreted as Inverse Compton emission in the Cosmic Microwave Background, then it is consistent with a rather low magnetic field strength of $\approx 11\mu$G,[32] independently of distance, etc., given the observed nonthermal X-ray flux as synchrotron emission from the same electrons. Whether the γ-ray emission could also be due to π^0-decay is an open question, given all the uncertainties. However, if the remnant was indeed as distant as 6 kpc, then the π^0-decay flux would be negligible compared to the observed flux. If, in addition the SNR shock still propagated in the rarefied wind bubble of a massive star, then the π^0-decay flux should be significantly reduced due to the dilution effect in the bubble[34]. A lot more work must be done before this extraordinary source is clearly understood.

3.3 Tycho's SNR in the Northern Sky

The progenitor of this SN type Ia was probably situated in a more or less uniform environment, making it another "astronomically simple" object, like SN 1006 in the South. Although the observed X-ray continuum between 10 and 20 keV[35] from RXTE may be interpreted as synchrotron emission (see however [36] for a different view), the X-ray flux is in general dominated by line emission which suggests that IC γ-ray emission is not the dominant contributor to the expected TeV γ-ray flux. In many ways Tycho should be the prototype of a recently born CR source in the Galaxy. An earlier attempt to detect it was made by the Whipple group which, after an observation time of ~ 14 hrs, could set an upper limit to the flux at 300 GeV[39]. More recently the HEGRA stereoscopic system has observed the source for ~ 65 hours at energies above 1 TeV[53]. No significant γ-ray flux was detected either, leading to an upper limit of 5.78×10^{-13}ph cm^{-2} sec^{-1} above 1 TeV, roughly 4 times lower than the Whipple upper limit if the different energy is accounted for. If the radio and the keV flux are

interpreted as synchrotron radiation, then the non-observation of a corresponding IC γ-ray flux implies a lower limit to the magnetic field strength of about 20μG. Using the analysis of the ASCA detection[37], on the other hand, weakens such an upper limit to about 6μG. Although on the high side for an unperturbed upstream interstellar field, even a 20μG field strength might actually exist, a 6μG field is in any case possible .

The hadronic γ-ray flux predictions[53], rescaled from[15] and renormalised cf. section 2, give a result that is equally close to the deduced upper limit: The experimental results appear however to exclude high injection rates, $\eta = 10^{-3}$, cases (a) and (b) in Fig. 7. Disregarding the rather unphysical case (d) that assumes a constant mean ejecta velocity, the upper limit is only slightly above the low injection case (c), with $\eta = 10^{-4}$.

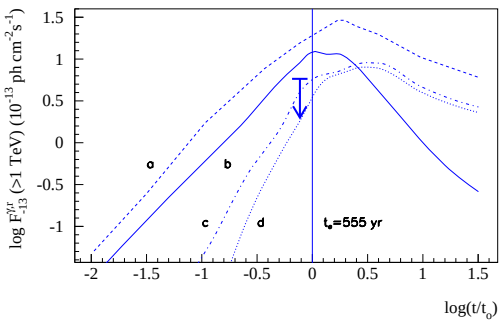

Figure 7: Time dependent calculation of the π^0-decay γ-ray flux for Tycho's SNR for four different parameter sets: dashed line, case a) $\eta = 10^{-3}$ and $B = 5\mu$G; solid line, case b) $\eta = 10^{-3}$ and $B = 30\mu$G; dash-dotted line, case c) $\eta = 10^{-4}$ and $B = 5\mu$G; dotted line, case d) is a single velocity ejecta case with $\eta = 10^{-4}$ and $B = 5$

Therefore, the γ-ray observations of Tycho's SNR come so close to theoretical predictions that a deeper observation, like it will be possible with the VERITAS array or the MAGIC telescope, should indeed lead to a detection, even taking into account the general astronomical uncertainties in distance, ambient density and total energy that exist also for this object.

3.4 Cassiopeia A in the Northern Hemisphere

Cas A is presumably the youngest known SNR in the Galaxy, dating back to about 1680, and the strongest radio source in the sky. It has been detected in TeV γ-rays in the deepest γ-ray observation up to now[38] at a level of ~ 3 % of the Crab flux. The observations are described in these Proceedings[40]. If besides the radio continuum also the hard X-ray flux [17] is interpreted as synchrotron emission [56], see Fig. 8, a corresponding γ-ray emission due to Bremsstrahlung and IC scattering should result. The existing observational results are compared with model predictions in Fig. 9. The magnetic field strengths assumed are in the ~ 1 mG range, whereas the implied matter density corresponds to 15 H-atoms cm^{-3}. A total energy in protons $W_p = 2 \times 10^{49}$ erg was assumed, for a proton differential spectral index of 2.15 and a cutoff energy of 100 TeV. The higher extension in energy, expected for the nucleonic spectrum, slightly favors a nucleonic origin for the γ-ray emission.

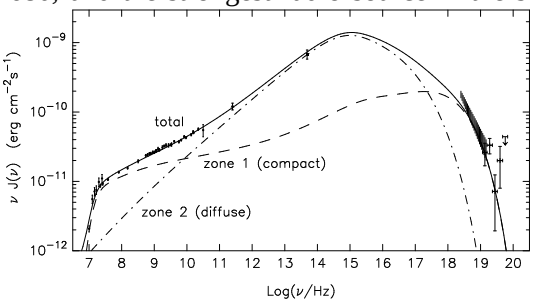

Figure 8: Model for the synchrotron SED for Cas A. The inhomogeneous remnant is divided into 2 components (zones), where zone 1 comprises the many small-scale features, assumed to be sources of energetic particles, and the remaining diffuse emission region (zone 2) fed by zone 1 sources and the outer SNR shock. A good fit to the data points is obtained

Recently, Laming [42] has argued that the hard X-ray emission could also be Bremsstrahlung from nonthermal electrons with several tens of keV, energised by lower hybrid waves from shock reflected ions at quasi-perpendicular shocks. Such a mechanism had been first suggested by [43]. Since the progenitor of Cas A is presumably a massive, fast-rotating Wolf-Rayet star in whose Red Supergiant wind the SNR shock is presently propagating [44], the shock may indeed be largely quasi-perpendicular. If this latter electron energisation scenario produces enough energy to yield the observed Bremsstrahlung, the detection of Cas A in γ-rays would necessarily imply a dominant hadronic γ-ray production! Moreover, the effect opens the Pandora box also for SNe of the type Ia like Tycho, or even SN 1006, in that a relevant fraction of the observed hard X-ray continuum could be nonthermal bremsstrahlung due to the partly quasi-perpendicular nature of the SNR shock in a uniform external magnetic field (section 2.2). This would clearly shift the interpretation towards an increasing nucleonic γ-ray fraction in general.

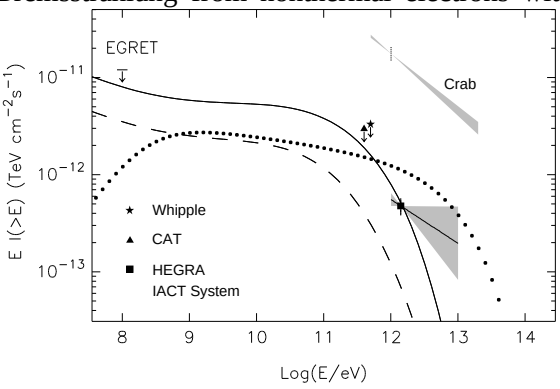

Figure 9: Measured flux and spectral index of Cas A in the context of model predictions. Shaded area shows 1σ error range for the spectral index. Solid and dashed lines show predicted IC plus bremsstrahlung flux for two different values of the B-field, whereas the dotted line shows a possible form for the hadronic γ-ray flux. Also indicated are the upper limits measured by EGRET, Whipple and CAT, and the values for the Crab Nebula.

4 Older core collapse SNRs in TeV γ-rays

Several older core collapse SNRs have been observed as well, and none of them could be detected in TeV γ-rays [39,45,49], even though they had been detected in GeV γ-rays by the EGRET instrument. We shall concentrate here on γ-Cygni and IC 443, since both the Wipple and the HEGRA telescopes have observed them. Even if the upper limits would have corresponded to detections, a naive straight line interpolation between the EGRET and the TeV fluxes would not correspond to the expected CR source spectrum but rather to one that is considerably steeper.

In the case of γ-Cygni also the EGRET error circle is fully inside and much smaller than the radio shell that marks the SNR morphology. Therefore the EGRET source cannot be the shell SNR. In fact, later X-ray measurements[47] have indicated the presence of a young pulsar, although the discussion is not really closed[26].

IC 443 is a more complex case. In contrast to γ-Cygni, this remnant appears indeed to be interacting with dense cloud material, as indicated by the presence of OH maser emission[46]. However, the X-ray emission is again characterised by localised patches, partly outside the EGRET error circle, and not delineating a uniformly illuminating if inhomogeneous shell remnant. The expected π^0-decay γ-ray flux is, within the considerable uncertainties of the astronomical parameters, about equal to the Whipple and HEGRA upper limits. Therefore a deeper γ-ray observation might well lead to a TeV detection.

From the point of view of acceleration theory both SNRs might possibly also be

rather rare and older so-called Wind-Supernovae, where the SNR shock is outside the stellar wind region of the massive progenitor but still inside the low-density, hot bubble of shocked wind material. It is expected that such objects exhibit a low γ-ray emission of nucleonic origin, and presumably a low IC/Bremsstrahlung emission as well [34].

Even though the experimental situation is not fully clarified, these sources are complex enough in every respect that it is difficult to draw any firm conclusions at present. This has not prevented rather pessimistic reactions, either observationally [39], or theoretically [48]. The prime lesson we can learn from these examples is probably that SNRs have very individual characteristics, far from being simple templates like low-mass main sequence stars.

5 Diffuse γ-ray emission from the Galactic disk

EGRET observations have shown an enhanced γ-ray emission from the Galactic disk above a few GeV in comparison with the standard models which otherwise describe the spectral intensity and γ-ray morphology of the disk fairly well [50]. This hardening of the energy spectrum, which is particularly pronounced near the disk's midplane, might be due to CR propagation effects, e.g. [54, 55]. An interesting alternative is its origin in the hard spectrum of γ-ray production *inside* SNRs if these SNRs contribute a sufficiently strong unresolved background of CR sources in the disk. Estimates [51] have shown that this should indeed be the case, the source contribution dominating above ~ 100 GeV.

Recent HEGRA observations have not detected a diffuse γ-ray background in the Galactic disk above 1 TeV [52]. However, they have been able to establish an upper limit which lies only a factor of ~ 2 above the predicted emission from the unresolved ensemble of CR sources in the form of SNRs. If this was indeed the case, then deeper observations with the upcoming arrays H.E.S.S. and CANGAROO in the Southern Hemisphere should be able to detect this background and thus to establish the *average* form of the Galactic CR source spectrum due to SNRs. Furthermore, a TeV-detection of the radial γ-ray distribution in the Galaxy would be a complementary result, allowing a direct comparison with the SNR distribution inferred from radio measurements.

6 Conclusions

SNRs are complex nonthermal objects, often situated in a disturbed environment, and they defy oversimplified quantitative theoretical as well as – in many cases – observational interpretations. On the other hand, they are the only nonthermal astrophysical sources for which something exists what one might call a real theory in the first place, even if it is not complete as we have seen. The sensitivity of present γ-ray detectors is still marginal for the detection of such objects [24]. We have argued that the existing, in their majority unsuccessful, observational searches are nevertheless consistent with theoretical expectations. For the detected remnants it is difficult to seperate the γ-ray fluxes of nucleonic and of electronic origin. For this reason, and for the fact that none of the three claimed detections has yet been confirmed by independent measurements, the question of a SNR origin of the Galactic CRs below the "knee" remains open. We have, however, also pointed out, how close some of the most recent observational results are to the corresponding theoretical flux estimates. This gives the next generation of γ-ray detectors a decisive role. Let us see what the experiment says!

1. M.G. Baring, D.C. Ellison, F.C. Jones, ApJ Suppl. **90**, 547 (1994).
2. L. Bennett, D.C. Ellison, J. Geophys. Res. **100**, A3, 3439 (1995).
3. M.A. Malkov, H.J. Völk, A&A **300**, 605 (1995).
4. M.A. Malkov, ApJ **485**, 638 (1995).
5. M.A. Malkov, Phys. Rev E **58**, No. 4, 4911 (1998).
6. M.A. Malkov, H.J. Völk, Adv. Space Res. **21**, No. 4, 551 (1998).
7. M.A. Malkov, L. O'C. Drury, Rep. Prog. Phys. **64**, 429 (2001).
8. M. Scholer, H. Kucharek, K.J. Trattner, Adv. Space Res. **21**, 533 (1998).
9. A.R. Bell, MNRAS **182**, 147 (1978)
10. L.O'C. Drury, Rep. Prog. Phys. **46**, 973 (1983).
11. R.D. Blandford, D. Eichler, Phys. Rep. **154**, 1 (1987).
12. E.G. Berezhko, G.F. Krymsky, Sov. Phys.-Uspekhi. **12**, 155 (1988).
13. A. Mastichiadis, A&A **305**, L53 (1996).
14. E.G. Berezhko, V.K. Yelshin, L.T. Ksenofontov, Astropart. Phys. **2**, 215 (1994).
15. E.G. Berezhko, H.J. Völk, Astropart. Phys. **7**, 183 (1997).
16. K. Koyama, R. Petre, E.V. Gotthelf, U. Hwang, M. Matsura, M. Ozaki, S.S. Holt, Nature **378**, 255 (1995).
17. G. Allen, et al., ApJ **487**, L97 (1997).
18. D. C. Ellison, S.P. Reynolds, ApJ **382**, 242 (1991).
19. P. Duffy, L. Ball, J.G. Kirk , ApJ **447**, 364 (1995).
20. S.P. Reynolds, ApJ **459**, L13 (1996).
21. M. Pohl, A&A **307**, 57 (1996).
22. A. Mastichiadis, O.C. de Jager, A&A **311**, L5 (1996).
23. T. Yoshida, S. Yanagita, in: Proc. 2nd INTEGRAL Workshop "Transparent Universe", ESA SP-382, 85 (1997).
24. L.O'C. Drury, F.A. Aharonian, H.J. Völk, A&A **287**, 959 (1994).
25. T. Naito, F. Takahara, J. Phys. G **20**, 477 (1994).
26. H.J. Völk, in: O.C. de Jager (ed.) Proc "Towards a Major Atmospheric Cherenkov Detector-V", Kruger National Park, 87 (1997).
27. E.G. Berezhko, L.T. Ksenofontov, S.I. Petukhov, Proc. 26th Int. Cosmic Ray Conf. (Salt Lake City) **3**, 431 (1999).
28. F.A. Aharonian, A.M. Atoyan, A&A **351**, 330 (1999).
29. K. Koyama, et al., PASJ **49**, L7 (1997).
30. P. Slane, B.M. Gaensler, T.M. Dame, J.P. Hughes, P.P.Plucinsky, A. Green, ApJ **525**, 357 (1999).
31. T. Tanimori, Y. Hayami, S. Kamei, et al., ApJ **497**, L25 (1998).
32. H. Muraishi,T. Tanimori, S. Yanagita, et al., A&A **354**, L57 (2000).
33. E. Pfeffermann, B. Aschenbach, in: "Roentgenstrahlung from the Universe", MPE Rep. **263**, 267 (1996).
34. E.G. Berezhko, H.J. Völk, A&A **357**, 283 (2000).
35. R. Petre, G.E. Allen, U. Hwang, Astron. Nachrichten **320**, 199 (1999).
36. J.M. Laming, ApJ **499**, 309 (1998).
37. U. Hwang, J.P. Hughes, R. Petre ApJ **497**, 833 (1998).
38. F.A. Aharonian, A.G. Akhperjanian, J.A. Barrio, et al., A&A, to appear (2001).
39. J.H. Buckley, C.W. Akerlof, D.A. Carter-Lewis, et al., A&A **329**, 639 (1998).
40. D. Horns, these Proceedings.
41. A.M. Atoyan, R.J. Tuffs, F.A. Aharonian, H.J. Völk, A&A **354**, 915 (2000).

42. J.M. Laming, ApJ **546**, 1149 (2001).
43. A.A. Galeev, Sov. Phys. JETP **86**, 1655 (1984).
44. K.J. Borkowsky, A.E. Szymkowiak, J.M. Blondin, C.L. Sarazin, ApJ **466**, 866 (1996).
45. M. Hess (HEGRA collaboration), Proc. 25th ICRC (Durban) **3**, 229 (1997).
46. M.J. Claussen, D.A. Frail, W.M. Goss, R.A. Gaume, ApJ **489**, 143 (1997).
47. K.T.S. Brazier, G. Kanbach, A. Carraminana, J. Guichard, M. Merck, MNRAS **281**, 1033 (1996).
48. J.G. Kirk, R.O. Dendy, J. Phys. G, in press (2001).
49. G.P. Rowell, T. Naito, S.A. Dazely, et al., A&A **359**, 337 (2000).
50. S.D. Hunter, et al., ApJ **481**, 205 (1997).
51. E.G. Berezhko, H.J. Völk, ApJ **540**, 923 (2000).
52. F.A. Aharonian, A.G. Akhperjanian, J.A. Barrio, et al., A&A submitted (2001).
53. F.A. Aharonian, A.G. Akhperjanian, J.A. Barrio, et al., to appear in A&A (2001).
54. F.A. Aharonian, A.M. Atoyan, A&A **362**, 937 (2000).
55. H.J. Völk, in: AIP Conf. Proc. 515, “GeV – TeV Gamma Ray Astrophysics Workshop: Towards a Major Atmospheric Cherenkov Detector VI”, ed. B.L. Dingus, M.H. Salamon, & D.B. Kieda (New York: AIP), 281 (2000)
56. A.M. Atoyan, F.A. Aharonian, R.J. Tuffs, H.J. Völk, A&A **355**, 211 (2000).